**IAES International Journal of Robotics and Automation (IJRA)**
Vol. 15, No. 2, June 2026, pp. 295~306
ISSN: 2722-2586, DOI: 10.11591/ijra.v15i2.pp295-306 

# LiDAR-based sensor fusion and navigation for indoor autonomous mobile robots in warehouse environments

**Rifda Hakima Sari, Jazi Eko Istiyanto, Oskar Natan, Zaidan Hakim, Danang Lelono, Andi Dharmawan**
Department of Computer Science and Electronics, Universitas Gadjah Mada, Yogyakarta, Indonesia

**Article Info**

***Article history:***

Received Dec 20, 2025
Revised Mar 13, 2026
Accepted Apr 1, 2026

***Keywords:***

Autonomous mobile robot
Path planning
Sensor fusion
SLAM
Warehouse automation

**ABSTRACT**

An indoor navigation system for an autonomous mobile robot was developed using LiDAR-based perception and multi-sensor fusion. The system combines 2D LiDAR, inertial measurement unit (IMU), and wheel encoder measurements within a simultaneous localization and mapping (SLAM) framework to support real-time localization, while the ROS2 Nav2 stack manages global path planning and local obstacle avoidance through A*-based planning and costmap-driven control. Evaluation in a warehouse-like environment showed that the robot maintained stable localization with low drift and completed autonomous navigation missions with a success rate of 93.33%. During operation, the robot was able to avoid static obstacles consistently and adjust its trajectory in response to simple dynamic obstacles through online replanning. These results indicate that the proposed system is suitable for practical indoor logistics scenarios requiring reliable navigation in structured environments. At the same time, the findings suggest the need for further improvement to handle environments with higher dynamics and denser obstacle configurations.



***Corresponding Author:***

Jazi Eko Istiyanto
Department of Computer Science and Electronics, Universitas Gadjah Mada
Sleman Regency, Special Region of Yogyakarta, Indonesia
Email: jazi@ugm.ac.id

## 1. INTRODUCTION

The increasing adoption of Industry 4.0 technologies has accelerated the use of automation in logistics and warehousing, particularly through autonomous mobile robots (AMRs) for material handling and repetitive indoor transport tasks [1]. In warehouse environments, robots are expected to travel across long corridors, operate continuously, and maintain reliable navigation performance under repetitive and time-sensitive working conditions [2]. These operational requirements place strong demands on localization accuracy, path planning, and obstacle avoidance, making indoor navigation one of the key technical challenges in mobile robotics.

Reliable navigation in indoor environments remains difficult when AMRs depend on a single sensing modality. Wheel odometry provides continuous motion feedback, but its estimation error accumulates over time due to wheel slip and surface irregularities [3], [4]. Similarly, standalone 2D LiDAR may experience degraded localization performance in feature-sparse or geometrically repetitive environments, such as warehouse corridors with similar scan patterns [5]. Although visual simultaneous localization and mapping (SLAM) and 3D LiDAR-based approaches can improve environmental perception and localization accuracy, such methods generally require more expensive hardware and greater computational resources, which may reduce their practicality for scalable warehouse deployment [6]. For this reason, a navigation framework that combines robust localization with affordable sensing and real-time computation remains highly relevant for indoor AMR applications.

Recent research in indoor robot navigation has explored both LiDAR-based and multi-sensor approaches. LiDAR-based SLAM continues to be widely used in indoor robotic systems because it offers practical deployment and relatively low computational demand compared with richer vision-based approaches [7]. At the same time, multi-sensor fusion has been recognized as an effective way to improve localization reliability by combining complementary measurements from different sensing modalities [8]. Related studies have shown that sensor fusion can support map construction, state estimation, and path planning in mobile robots [9], [10], while other works have highlighted the limitations of systems that rely only on obstacle avoidance or on computationally intensive sensing configurations [11]–[14]. Taken together, these findings suggest that low-cost sensor fusion remains a promising direction, especially for warehouse robots that must navigate structured yet dynamic indoor spaces.

Based on this motivation, this study develops an indoor AMR navigation system by integrating 2D LiDAR, an inertial measurement unit (IMU), and wheel encoder data within the ROS2 Nav2 framework. The proposed system uses an extended Kalman filter (EKF) to combine the complementary strengths of the three sensors, where LiDAR provides environmental perception, the IMU contributes orientation and motion information, and the encoders provide short-term displacement feedback. This integration is intended to reduce odometric drift, improve localization consistency, and maintain stable navigation performance when the robot encounters corridor-scale motion, repetitive environmental structures, and changing obstacle conditions.

The contribution of this work lies in the implementation of low-cost and computationally efficient sensor-fusion architecture for indoor AMR navigation in warehouse-like environments. First, this study develops a multi-sensor localization framework using 2D LiDAR, IMU, and wheel encoder data to improve pose estimation reliability. Second, the framework is integrated with ROS2 Nav2 to support global path planning, local obstacle avoidance, and real-time replanning. Third, the study demonstrates the applicability of the proposed system in structured indoor navigation tasks involving both static and dynamic obstacles. Through this combination, the work aims to provide a practical navigation solution for warehouse AMRs that require dependable operation without relying on high-end sensing platforms.

## 2. RESEARCH METHOD

This chapter describes the methodology adopted to develop and validate the AMR system. The system design and implementation involve the integration of multiple components, including LiDAR, IMU, wheel encoders, and onboard computing units. In addition, this chapter explains the overall system architecture, the sensor fusion approach, the path planning methods, and the experimental setup used to assess the AMR's performance.

### 2.1. Mathematical modelling and state estimation

For localization analysis, the robot is treated as a mobile platform operating on a two-dimensional plane, with its pose defined by the state vector $\mathrm{x}_k = [x_k, y_k, \theta_k]^\top$. Here, $x_k$ and $y_k$ denote the robot position in the global map frame, and $\theta_k$ is the heading angle at discrete time step $k$. This representation is consistent with the pose variables required for map-based navigation, global planning, and closed-loop path execution [15]. The robot motion is formulated using a differential-drive kinematic model. When expressed in terms of body-frame linear and angular velocities $\mathrm{u}_k = [v_k, \omega_k]^\top$, the discrete-time propagation can be written as (1).

$$\mathrm{x}_{k+1} = \begin{bmatrix} x_k + v_k \Delta t \cos(\theta_k) \\ y_k + v_k \Delta t \sin(\theta_k) \\ \theta_k + \omega_k \Delta t \end{bmatrix} + \mathrm{w}_k \quad (1)$$

where $\Delta t$ is the sampling period and $\mathrm{w}_k$ is process noise capturing wheel slip and modelling uncertainty. Alternatively, when using wheel encoder increments directly, the incremental motion can be formulated by $\Delta s = (\Delta s_r + \Delta s_l)/2$ and $\Delta\theta = (\Delta s_r - \Delta s_l)/b$, where $\Delta s_r$ and $\Delta s_l$ are the right and left wheel travel distances, respectively, and $b$ is the wheelbase [16]. The pose update is then expressed from (2),

$$x_{k+1} = x_k + \Delta s \cos\left(\theta_k + \frac{\Delta\theta}{2}\right), y_{k+1} = y_k + \Delta s \sin\left(\theta_k + \frac{\Delta\theta}{2}\right), \theta_{k+1} = \theta_k + \Delta\theta \quad (2)$$

which provides a practical formulation for odometry-driven state propagation during navigation.

To relate the robot state to sensor observations, a measurement model is defined to describe how perceived features constrain the pose estimate. For example, given a landmark or map feature located at $\mathrm{p}_\ell = [x_\ell, y_\ell]^\top$, a common range bearing observation model is shown by (3).

$$z_k = \begin{bmatrix} r_k \\ \phi_k \end{bmatrix} = \begin{bmatrix} \sqrt{(x_\ell - x_k)^2 + (y_\ell - y_k)^2} \\ \text{atan2}(y_\ell - y_k,\, x_\ell - x_k) - \theta_k \end{bmatrix} + v_k \quad (3)$$

where $v_k$ is zero-mean measurement noise. In practice, LiDAR measurements provide dense geometric constraints against the occupancy map, and the same principle applies: the pose estimate is updated by maximizing the consistency between the predicted observation (from the map and pose) and the actual scan, which is essential for robust indoor localization [17].

Together, the motion and measurement models establish the basis for probabilistic pose estimation during autonomous navigation. The motion model governs how the pose evolves from odometry, while the observation model constrains the pose using LiDAR–map consistency; together they support stable estimation of $(x, y, \theta)$ after mapping is completed and the robot navigates using the saved 2D occupancy grid map. As a result, the downstream modules such as global path planning, local obstacle-aware motion generation, and path following operate on a pose estimate that remains reliable despite drift sources such as wheel slip or transient sensor noise [18].

### 2.2. Hardware architecture

The proposed AMR employs a differential-drive mobile platform for indoor warehouse logistics. The hardware system integrates sensing, computation, power management, and actuation modules to support real-time localization and navigation. Figure 1 presents the overall hardware overview of the proposed system, including the system architecture and the physical robot platform. As shown in Figure 1(a), the hardware architecture defines the flow of power and data among the sensing, processing, and actuation units. The NVIDIA Jetson AGX Orin serves as the onboard computing platform for real-time sensor processing and ROS2-based navigation. Sensor data are acquired from the RPLIDAR A1, the BNO055 IMU, and wheel encoders. The RPLIDAR A1 is used as the main perception sensor because its 0.5° angular resolution is sufficient for planar mapping in structured indoor environments while maintaining lower cost and complexity than 3D LiDAR alternatives.

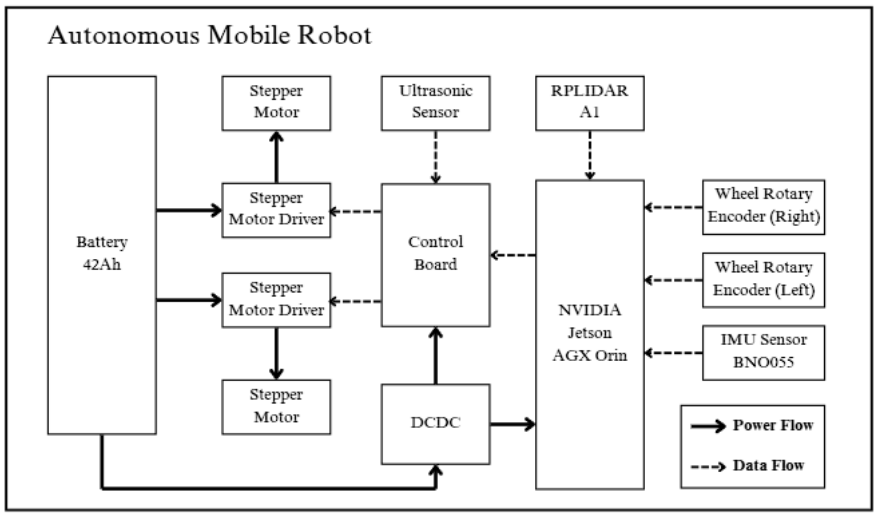


(a)

(b)

Figure 1. Hardware overview of the proposed AMR System: (a) system architecture and (b) physical implementation of the robot platform

Figure 1(b) shows the physical implementation of the robot platform used in the experiments. The AMR is built as a compact, low-profile mobile base suitable for confined indoor spaces such as warehouse corridors. The battery pack, computing unit, sensing modules, and motor drivers are integrated within the chassis to improve mechanical stability and simplify deployment. Power is supplied by a 42 Ah battery and regulated through a DC-DC converter to provide stable voltage for the onboard computer, sensors, and control electronics, thereby reducing the risk of voltage drops during high-load motor operation. The control board functions as the communication interface among the sensors, computing unit, and peripheral devices, while also transmitting motion commands to the motor drivers.

LiDAR measurements are used for mapping and localization within the SLAM process [19]. The IMU provides orientation and angular motion information to improve pose estimation, while wheel encoders supply rotational feedback for estimating linear displacement and supporting localization and path-planning functions [20].

### 2.3. Sensor fusion and localization

The AMR localization process is based on the combined use of LiDAR, IMU, and wheel encoder measurements to obtain a more reliable estimate of the robot pose. In the proposed system, these sensor streams are processed within the SLAM module, which is responsible for both map generation and odometry estimation, as illustrated in Figure 2. LiDAR data provide a 360-degree representation of the surrounding environment and serve as the main input for mapping and object detection [21]. This information is used by the SLAM module to construct the environmental map and estimate the robot position within that map. Nevertheless, LiDAR measurements may be affected by sensor noise and environmental disturbances [22], [23]. To improve pose consistency, the IMU contributes orientation information, including pitch, roll, and yaw, which is particularly useful during robot motion and turning maneuvers [24]. In parallel, the wheel encoders provide displacement-related odometry data based on wheel rotation along the traveled path.

To reduce the effect of uncertainty from each sensing modality, the proposed system applies a sensor-fusion approach to combine LiDAR, IMU, and encoder data [25]. This fusion process is implemented using an Extended Kalman Filter (EKF), which estimates the robot state from the complementary information provided by the three sensors. As shown in Figure 2, the fused measurements are used by the SLAM Toolbox to improve real-time localization and support consistent map construction during operation. Through this data flow, the AMR is able to update its pose and map continuously, allowing the system to maintain reliable navigation performance under dynamic indoor conditions.

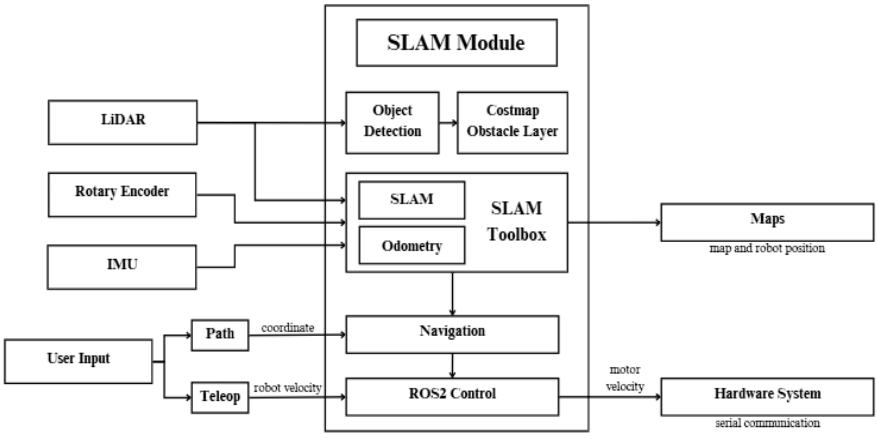


Figure 2. Sensor fusion and localization: integration of LiDAR, IMU, and encoder

### 2.4. Navigation architecture

Figure 3 summarizes the operating logic of the proposed AMR navigation system during autonomous operation. Following system initialization, the robot enters the mapping stage to generate a spatial representation of the environment. The resulting map is then checked for navigation suitability, and the robot continues exploration until a valid 2D occupancy grid map is obtained and stored.

The lower part of the flowchart represents the navigation loop during path following, where local planning and obstacle monitoring are performed continuously. When an obstacle is detected, the system activates local replanning or recovery behavior to maintain safe motion. Otherwise, the robot continues following the planned route until the target is reached and the navigation task is completed.

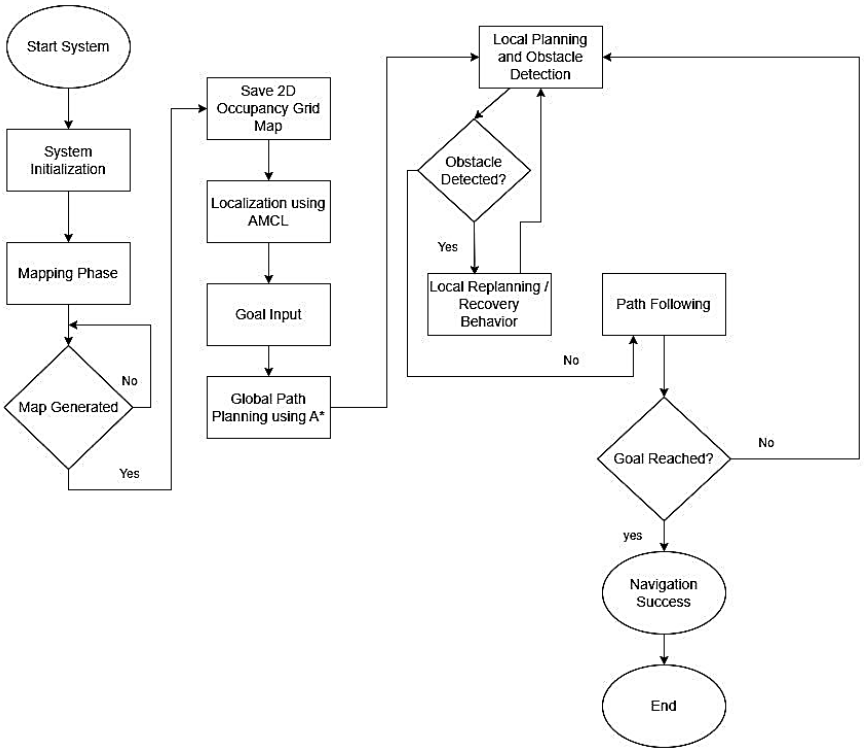


Figure 3. Operational flowchart of the autonomous navigation System

Figure 4 presents the navigation control architecture of the proposed AMR system. Sensor observations and state estimates are transformed into motion commands through an integrated pipeline consisting of localization, global planning, local planning, and low-level actuation. A target pose is used as the navigation goal, and the system continuously updates its planning and control actions based on real-time sensor feedback and odometry data.

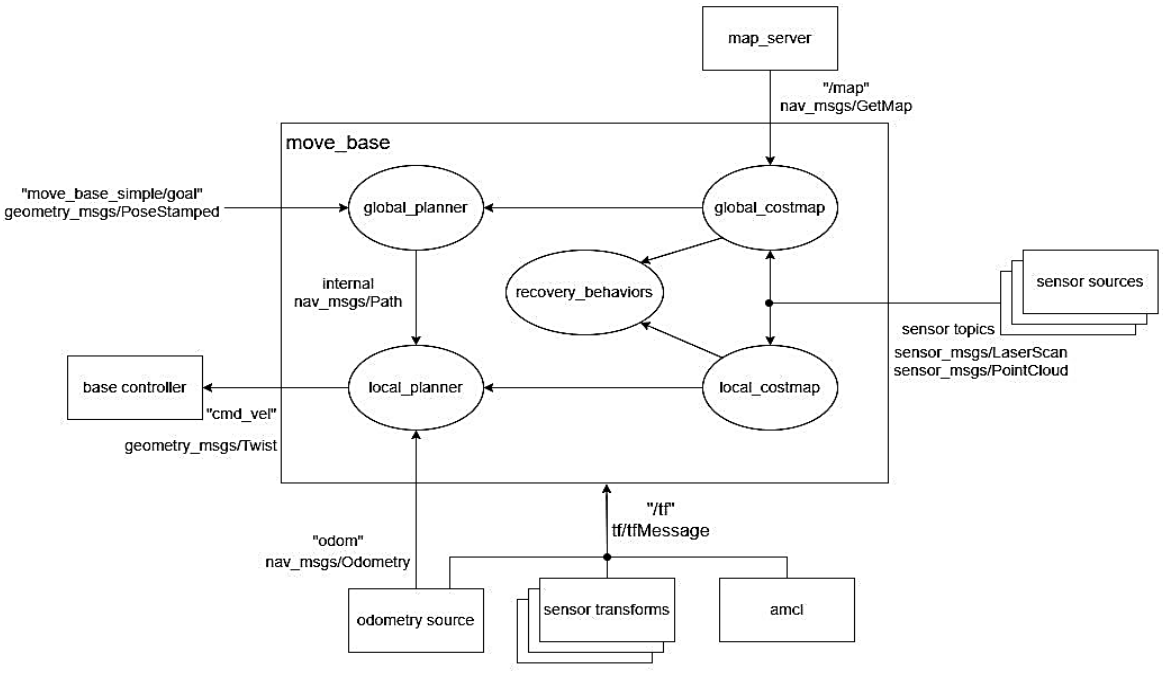


Figure 4. System-level navigation control diagram

After the mapping phase produces an occupancy grid map, the AMR enters localization-navigation mode using the stored map as a fixed global reference. The robot pose $(\theta)$ is estimated through adaptive Monte Carlo localization (AMCL), which updates multiple pose hypotheses by matching LiDAR observations to the map [26]. Wheel-encoder odometry propagates motion between updates, while the transform chain maintains consistency among the robot, odometry, and map frames. This probabilistic localization process reduces odometry drift and provides a stable pose estimate for planning [27].

Using the estimated pose and global map, the system computes a feasible route to the navigation goal. The global planner applies the A* algorithm to the static occupancy grid to generate a path that avoids non-traversable regions and satisfies corridor constraints. During execution, a local costmap is updated from real-time sensor data to represent nearby obstacles and safety margins. The local planner follows the global path while generating velocity commands that satisfy the robot's kinematic constraints and avoid collisions. When unexpected obstacles or blocked passages are encountered, recovery behaviors are activated to restore a feasible navigation state and enable replanning when necessary [28], [29]. The resulting commands are sent to the base controller, which converts them into actuator-level signals for the drive system and maintains continuous closed-loop navigation.

### 2.5. Experimental setup

To validate the proposed system, experiments were conducted in the Embedded Systems and Robotics Laboratory, Universitas Gadjah Mada, which was configured to mimic a warehouse layout. The environment featured several narrow corridors and open areas. Typical laboratory equipment, such as desks and storage racks, were utilized as obstacles to simulate the constrained spaces found in industrial settings.

The navigation performance was evaluated under two primary testing scenarios.

- Static Obstacle Avoidance: Fixed objects, including chairs and vertical boards, were placed directly along the planned path to evaluate the local planner's ability to generate alternative trajectories.
- Dynamic Obstacle Interaction: To test the system's responsiveness to unpredictable changes, a person crossed the robot's path at a standard walking speed, requiring the dynamic obstacle layer in the costmap to trigger online replanning.

For quantitative localization analysis, ground truth measurements were obtained by comparing the robot's estimated pose against reference positions manually measured at predefined waypoints along the test route. These waypoints provided the necessary data to calculate the Root Mean Square Error (RMSE) for both planar position and orientation.

This study evaluates the path-planning and obstacle-avoidance performance of the Autonomous Mobile Robot (AMR) in a controlled indoor environment. Prior to the navigation experiments, an initial mapping procedure is conducted to generate a spatial representation of the surrounding area. Figure 5 presents the overall path-planning visualization of the proposed AMR system. In particular, Figure 5(a) shows the occupancy grid map obtained during the mapping stage, which represents the structural layout of corridors and open spaces. The generated map is subsequently used as the global reference for localization and path planning, enabling the robot to identify traversable regions while avoiding non-navigable areas during autonomous operation [30].

Based on the generated map as a global reference, the AMR is tasked with moving from a predefined start position to a target location while avoiding both static and dynamic obstacles. The navigation framework combines global path planning with local obstacle avoidance, enabling the robot to generate an initial route and continuously adjust its motion in response to changes in the surrounding environment. The test environment is populated with various objects placed along the navigation corridor to emulate typical indoor obstacles, ensuring that the system is evaluated under realistic operating conditions.

During the test, the AMR's dynamic obstacle avoidance system was evaluated. The robot detects obstacles in its path and recalculates its trajectory accordingly, ensuring it avoids collisions while maintaining its path to the goal [31]. Figure 5(b) illustrates the robot trajectory during navigation, showing how the planned route is updated when obstacles are encountered. This behavior demonstrates the effectiveness of the implemented path-planning and obstacle-avoidance mechanisms.

In this study, the A* algorithm is employed to determine the optimal path for the robot by evaluating the cost function $f(n)$ at each node, as defined in (4).

$$f(n) = g(n) + h(n) \tag{4}$$

Here, $g(n)$ is the cost to reach the node from the start, and $h(n)$ is the estimated cost to reach the goal from the node, calculated using heuristics like Euclidean or Manhattan distance. The algorithm iterates through nodes, selecting the one with the lowest $f(n)$ value, and adjusts the path dynamically as the robot encounters new obstacles [32].

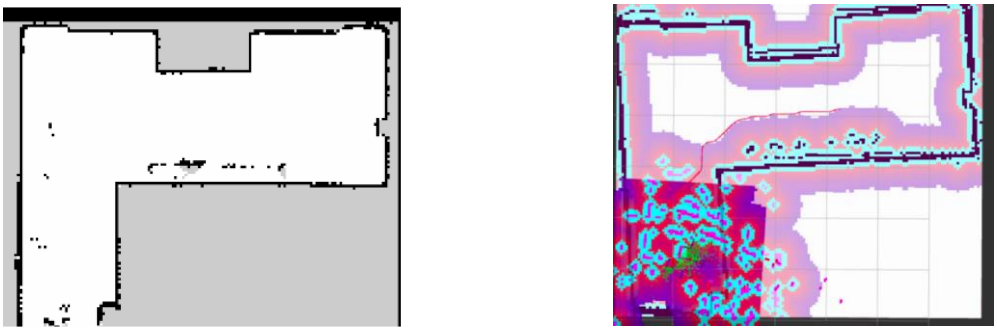

(a) (b)

Figure 5. Path planning visualization: (a) 2D occupancy grid map in indoor environment and (b) robot trajectory for dynamic obstacle avoidance

Through these tests, the system demonstrated a high success rate in following the planned path while avoiding obstacles. The path planning was robust, even when the robot encountered new or unexpected obstacles, and it maintained an efficient route to its goal.

## 3. RESULTS AND DISCUSSION

This chapter reports the experimental findings obtained from the evaluation of the proposed Autonomous Mobile Robot (AMR) system, with emphasis on its localization and navigation performance. The evaluation examines how effectively the robot follows planned trajectories, avoids obstacles, and maintains accurate real-time pose estimation using LiDAR, IMU, and wheel encoder data. Several test scenarios were conducted to examine the robustness of the proposed system under different operating conditions. The resulting data are analyzed in the following subsections to discuss the robot's response to varying obstacle configurations as well as the accuracy of its navigation and localization behavior.

### 3.1. Localization result

This section provides a quantitative assessment of the proposed localization system in the experimental warehouse environment. The accuracy of the multi-sensor fusion framework is evaluated by comparing the robot's estimated trajectory with ground-truth measurements. The analysis considers both translational and rotational errors in order to examine the ability of the system to limit drift during extended navigation. The resulting measurements reflect the consistency and precision of the SLAM-based localization process under real-time operating conditions.

#### 3.1.1. Robot Pose

The proposed AMR system was initially evaluated based on its ability to estimate the robot pose (θ) during navigation in the test arena. In this evaluation, the localization module fused LiDAR, wheel encoder, and IMU measurements to generate a continuous pose estimate, which was subsequently compared with reference positions obtained through manual measurements along a predefined path. This comparison was intended to determine whether the estimated pose produced by the localization algorithm remained sufficiently close to the actual robot position to support reliable autonomous navigation.

Table 1 summarizes the comparison between the pose commanded in the navigation program and the actual pose measured at several sample waypoints. The results show that the estimated positions in the map frame are consistently close to the reference values. The deviations in the $x$- and $y$- coordinates are on the order of a few centimetres, while the orientation error $\theta$ remains within a few degrees, with the largest deviation below approximately $10°$. These results indicate that the localization module can estimate the robot pose with sufficient accuracy for corridor-scale indoor navigation, and visually the trajectory of the robot follows the planned path without noticeable drift along the test route.

In addition to quantitative evaluation, the qualitative structure of the SLAM solution was examined using the global graph representation, as shown in Figure 6. This visualization overlays the robot's estimated trajectory and pose graph onto the generated environmental map. The consistent alignment of graph nodes and the absence of noticeable map deformation indicate that the back-end optimization effectively manages accumulated errors and preserves global map structure. The smoothness of the trajectory and the coherent loop closures provide further evidence that the system maintains stable localization over extended paths and throughout complex motions. Overall, both numerical and visual analyses confirm that the localization

module delivers dependable pose estimates suitable for real-time autonomous navigation in indoor environments. The stability of SLAM and the minimal drift observed across the test sequences support the effectiveness of the underlying sensor fusion approach and enable robust navigation performance.

Table 1. Robot pose test result

| Position in Program | | | Actual | | |
|---|---|---|---|---|---|
| x (m) | y (m) | θ (°) | x (m) | y (m) | θ (°) |
| 1 | 0 | -90 | 1.02 | 0.06 | -82 |
| 1.5 | 0 | -90 | 1.48 | 0.05 | -91 |
| 2 | 0 | -90 | 2.03 | 0.05 | -93 |
| 3 | 1 | 90 | 3.02 | 0.94 | 90 |
| 3 | 2 | 90 | 3.07 | 1.97 | 86 |
| 3 | 3 | 90 | 3.02 | 2.95 | 88 |
| 0 | 0 | 0 | 0.1 | 0 | 4 |

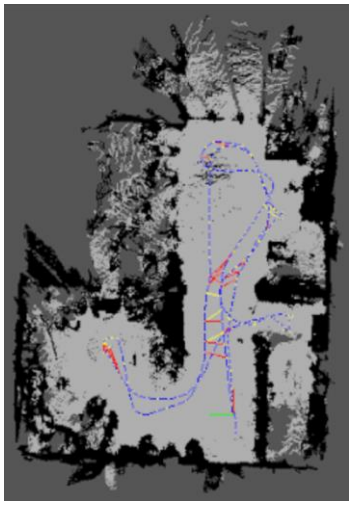

Figure 6. Global SLAM graph and estimated robot trajectory

### 3.1.2. Localization Error

To provide a more quantitative measure of localization accuracy, the Root Mean Square Error (RMSE) was computed from the pose comparison results summarized in Table 1 using the estimated and reference robot poses recorded during autonomous navigation. The RMSE was determined for the position components $(x, y)$as well as for the robot orientation $(\theta)$, based on the differences between the estimated poses and the corresponding reference measurements at multiple sampled locations. As summarized in Table 2, the RMSE values for the x- and y-position components are 0.050 m and 0.047 m, respectively, resulting in a combined planar position RMSE of 0.069 m. These results indicate that the localization error remains within a few centimeters throughout the navigation process. The orientation RMSE of 3.96° further demonstrates stable heading estimation during corridor-scale motion.

Table 2. Localization error using RMSE

| Metric | RMSE Value | Unit |
|---|---|---|
| RMSE Position (x) | 0.050 | m |
| RMSE Position (y) | 0.047 | m |
| RMSE Position (2D) | 0.069 | m |
| RMSE Orientation (θ) | 3.96 | degree |

From a practical navigation perspective, the obtained RMSE values are sufficiently low to support reliable autonomous operation in indoor environments. The level of positional and angular accuracy achieved enables consistent path following, safe obstacle clearance, and stable execution of navigation tasks without requiring external correction, thereby validating the robustness of the proposed localization system.

### 3.2. Navigation result

The path-planning and obstacle-avoidance performance of the AMR was examined through a series of autonomous navigation trials designed to represent warehouse operating conditions. In each trial, the robot was instructed to move from a predefined start pose to a target pose using the SLAM-generated map as the static global reference, while nearby obstacles were represented through a local costmap. The Nav2 stack computed a global path using the A* planner and continuously updated the local trajectory based on real-time sensor data. The resulting trajectory, visualized in Figure 6, shows that the robot follows the corridor layout and bends smoothly around occupied regions in the costmap, indicating that the planned path is consistent with the environment structure and avoids forbidden areas.

Mission-level performance is summarized in Table 3, which reports the outcome of 15 autonomous navigation trials under different combinations of start and goal poses. The AMR successfully reached the goal without collision in 14 of these trials, corresponding to a mission success rate of 93.33%, while 2 collisions were recorded. This result exceeds the predefined success criterion of at least 80% collision-free missions and demonstrates that the navigation stack is sufficiently reliable for typical indoor logistics operations, where repetitive and consistent navigation behavior is required. The few failure cases were associated with situations in which the robot approached tight passages and the local planner briefly selected trajectories that brought the robot too close to obstacles, suggesting that further tuning of the costmap inflation radius and obstacle cost parameters could further improve robustness.

Table 3. Navigation performance summary

| Number of Navigation Test | Success Rate (%) | Number of Collisions |
|---|---|---|
| 15 | 93.33 | 2 |

The obstacle avoidance behavior of the AMR was evaluated under both static and dynamic conditions to reflect realistic indoor scenarios. For static obstacles, fixed objects such as a chair and a vertical board were placed directly along the corridor between the start and goal positions. In these trials, the robot consistently detected the obstacles through the local costmap and generated alternative trajectories that routed around them, maintaining a minimum separation distance greater than the predefined safety threshold of 0.25 m. To further assess robustness, additional experiments were conducted in the presence of dynamic obstacles, including a person briefly crossing the robot's path and objects being repositioned during navigation. When such changes occurred, the local planner updated the costmap and triggered online replanning, causing the robot to reduce its speed, adjust its heading, and select a new collision-free trajectory while preserving the original goal. Qualitative inspection of the resulting paths indicates that the AMR was able to avoid both static and moving obstacles without becoming stuck or abandoning the mission, and it continued to complete navigation tasks within acceptable bounds of time and path length.

Overall, the experimental findings indicate that the proposed system is capable of generating safe and efficient navigation paths in both static and moderately dynamic indoor environments. The high mission success rate, respect for safety distance constraints, and ability to replan in response to moving obstacles indicate that the AMR is suitable for deployment in warehouse-like settings, where aisles may be partially obstructed and the environment can change during operation.

### 3.3. Result analysis

While the experimental results provide a strong indication of the system's baseline capabilities, a critical analysis reveals specific limitations regarding statistical significance and environmental complexity. First, the reported mission success rate of 93.33% must be interpreted within the context of the sample size of 15 trials. While this sample is sufficient to demonstrate the functional integration of the ROS2 Nav2 stack and the sensor fusion algorithm, it is not statistically exhaustive. The absence of a large-scale dataset prevents the calculation of narrow confidence intervals or rigorous hypothesis testing regarding long-term failure rates. Consequently, the claim of feasibility for practical indoor logistics applications is currently predicated on the assumption of controlled environmental variables. The system is validated for structured warehouse zones, but deployment in highly chaotic or unstructured industrial facilities would require further validation on a significantly larger scale to account for edge cases.

Furthermore, the evaluation of dynamic obstacle handling relied primarily on quantitative success/fail metrics and qualitative visual inspection of trajectory smoothness. While visual analysis confirms that the local planner successfully inflated costmaps and re-routed, it lacks the granularity to quantify the specific "social" efficiency or clearance margins in real-time. Finally, the reliance on 2D LiDAR constitutes a perception limitation in complex vertical environments.

## 4. CONCLUSION

This study examined the problem of reliable indoor navigation for autonomous mobile robots operating in warehouse-like environments. The proposed system integrates LiDAR-based perception and multi-sensor fusion within a unified framework that supports mapping, localization, and path planning for structured indoor operation. Experimental results demonstrate that the robot maintains stable localization and executes autonomous navigation tasks with a high level of reliability, achieving a navigation success rate of 93.33% while safely avoiding both static and dynamic obstacles. To build upon these findings, future research will focus on transitioning from 2D LiDAR sensor to RGB-D cameras, such as Intel RealSense D435i to enable more comprehensive 3D SLAM and semantic environment understanding. Additionally, further efforts will be directed toward optimizing the navigation architecture for more complex, multi-floor indoor layouts to expand its scalability in large-scale industrial applications.

## FUNDING INFORMATION

This work was supported by the Department of Computer Science and Electronics, Universitas Gadjah Mada under the Publication Funding Year 2026.

## AUTHOR CONTRIBUTIONS STATEMENT

This journal uses the Contributor Roles Taxonomy (CRediT) to recognize individual author contributions, reduce authorship disputes, and facilitate collaboration.

| Name of Author | C | M | So | Va | Fo | I | R | D | O | E | Vi | Su | P | Fu |
|---|---|---|---|---|---|---|---|---|---|---|---|---|---|---|
| Rifda Hakima Sari | | ✓ | ✓ | ✓ | ✓ | ✓ | ✓ | ✓ | ✓ | ✓ | ✓ | | ✓ | |
| Jazi Eko Istiyanto | | | | ✓ | ✓ | ✓ | | | | | | ✓ | ✓ | ✓ |
| Oskar Natan | ✓ | ✓ | | | | ✓ | ✓ | ✓ | | ✓ | | ✓ | ✓ | |
| Zaidan Hakim | ✓ | ✓ | ✓ | ✓ | | ✓ | ✓ | ✓ | ✓ | ✓ | ✓ | | ✓ | |
| Danang Lelono | ✓ | ✓ | | ✓ | ✓ | | | | | ✓ | | ✓ | ✓ | |
| Andi Dharmawan | ✓ | ✓ | | ✓ | ✓ | | | | | ✓ | | ✓ | ✓ | |

C : **C**onceptualization
M : **M**ethodology
So : **So**ftware
Va : **Va**lidation
Fo : **Fo**rmal analysis
I : **I**nvestigation
R : **R**esources
D : **D**ata Curation
O : Writing - **O**riginal Draft
E : Writing - Review & **E**diting
Vi : **Vi**sualization
Su : **Su**pervision
P : **P**roject administration
Fu : **Fu**nding acquisition

## CONFLICT OF INTEREST STATEMENT

Authors state no conflict of interest.

## DATA AVAILABILITY

The data will be made available on request.

## REFERENCES

[1] O. M. Çelik and M. Köseoğlu, "A modified Dijkstra algorithm for ROS-based autonomous mobile robots," *Journal of Advanced Research in Natural and Applied Sciences*, vol. 9, no. 1, pp. 205–217, Mar. 2023, doi: 10.28979/jarnas.1119957.

[2] L. Yang, Q. Bu, J. Sun, S. Liu, and F. Wang, "ROS2-based indoor autonomous navigation for moving obstacle avoidance," in *International Conference on Advanced Sensing and Intelligent Systems (ICASIS 2025)*, Oct. 2025, vol. 13808, p. 26. doi: 10.1117/12.3077477.

[3] L. Chang, X. Niu, and T. Liu, "GNSS/IMU/ODO/LiDAR-SLAM integrated navigation system using IMU/ODO pre-integration," *Sensors*, vol. 20, no. 17, p. 4702, Aug. 2020, doi: 10.3390/s20174702.

[4] Z. Chen, "Analysis of the application scenarios of different sensors in automated guided vehicles," *Highlights in Science, Engineering and Technology*, vol. 114, pp. 122–128, Oct. 2024, doi: 10.54097/n0an7570.

[5] Z. Jiang, "The application of SLAM technology in indoor navigation to complex indoor environments," in *AIP Conference Proceedings*, 2024, vol. 3144, no. 1, p. 030011. doi: 10.1063/5.0214220.

[6] I. G. Handono, O. Natan, A. Dharmawan, and N. P. Indarto, "Enhancing SLAM accuracy in urban dynamics: a novel approach with DynaVINS on real-world dataset," in *2025 10th International Conference on Control and Robotics Engineering (ICCRE)*, May 2025, pp. 160–164. doi: 10.1109/ICCRE65455.2025.11093488.

[7] H. Messbah, M. Emharraf, and M. Saber, "Robot indoor navigation: comparative analysis of LiDAR 2D and visual SLAM," *IAES International Journal of Robotics and Automation (IJRA)*, vol. 13, no. 1, p. 41, Mar. 2024, doi: 10.11591/ijra.v13i1.pp41-49.

[8] J. Klečka, K. Horák, and O. Boštík, "General concepts of multi-sensor data-fusion based SLAM," *IAES International Journal of Robotics and Automation (IJRA)*, vol. 9, no. 2, p. 63, Jun. 2020, doi: 10.11591/ijra.v9i2.pp63-72.
[9] A. Li, J. Cao, S. Li, Z. Huang, J. Wang, and G. Liu, "Map construction and path planning method for a mobile robot based on multi-sensor information fusion," *Applied Sciences*, vol. 12, no. 6, p. 2913, Mar. 2022, doi: 10.3390/app12062913.
[10] C. Debeunne and D. Vivet, "A review of visual-LiDAR fusion based simultaneous localization and mapping," *Sensors*, vol. 20, no. 7, p. 2068, Apr. 2020, doi: 10.3390/s20072068.
[11] C. Cadena *et al.*, "Past, present, and future of simultaneous localization and mapping: toward the robust-perception age," *IEEE Transactions on Robotics*, vol. 32, no. 6, pp. 1309–1332, Dec. 2016, doi: 10.1109/TRO.2016.2624754.
[12] F. Liu, Y. Cao, X. Cheng, and L. Liu, "A visual SLAM method assisted by IMU and deep learning in indoor dynamic blurred scenes," *Measurement Science and Technology*, vol. 35, no. 2, p. 025105, Feb. 2024, doi: 10.1088/1361-6501/ad03b9.
[13] M. Yang *et al.*, "Sensors and sensor fusion methodologies for indoor odometry: a review," *Polymers*, vol. 14, no. 10, p. 2019, May 2022, doi: 10.3390/polym14102019.
[14] R. Yuan, B. Ji, Y. Gao, and H. Tao, "A review of LiDAR simultaneous localization and mapping techniques for multi-robot," *Robotica*, vol. 43, no. 9, pp. 3200–3240, Sep. 2025, doi: 10.1017/S0263574725102178.
[15] S. Zheng, J. Wang, C. Rizos, W. Ding, and A. El-Mowafy, "Simultaneous localization and mapping (SLAM) for autonomous driving: concept and analysis," *Remote Sensing*, vol. 15, no. 4, p. 1156, Feb. 2023, doi: 10.3390/rs15041156.
[16] N. Rufus, U. K. R. Nair, A. V. S. S. B. Kumar, V. Madiraju, and K. M. Krishna, "SROM: simple real-time odometry and mapping using LiDAR data for autonomous vehicles," in *2020 IEEE Intelligent Vehicles Symposium (IV)*, Oct. 2020, pp. 1867–1872. doi: 10.1109/IV47402.2020.9304577.
[17] T. Shan, B. Englot, D. Meyers, W. Wang, C. Ratti, and D. Rus, "LIO-SAM: Tightly-coupled LiDAR inertial odometry via smoothing and mapping," in *2020 IEEE/RSJ International Conference on Intelligent Robots and Systems (IROS)*, Oct. 2020, pp. 5135–5142. doi: 10.1109/IROS45743.2020.9341176.
[18] R. H. Yuan, C. N. Taylor, and S. L. Nykl, "Accurate covariance estimation for pose data from iterative closest point algorithm," *NAVIGATION: Journal of the Institute of Navigation*, vol. 70, no. 2, p. navi.562, Mar. 2023, doi: 10.33012/navi.562.
[19] I. Filip, J. Pyo, M. Lee, and H. Joe, "LiDAR SLAM with a wheel encoder in a featureless tunnel environment," *Electronics*, vol. 12, no. 4, p. 1002, Feb. 2023, doi: 10.3390/electronics12041002.
[20] X. Niu, T. Yu, J. Tang, and L. Chang, "An online solution of LiDAR scan matching aided inertial navigation system for indoor mobile mapping," *Mobile Information Systems*, vol. 2017, pp. 1–11, 2017, doi: 10.1155/2017/4802159.
[21] B. Chen, H. Zhao, R. Zhu, and Y. Hu, "Marked-LIEO: visual marker-aided LiDAR/IMU/encoder integrated odometry," *Sensors*, vol. 22, no. 13, p. 4749, Jun. 2022, doi: 10.3390/s22134749.
[22] B. Wang, Q. Wu, Y. Liu, H. Zhang, X. Liu, and L. Pan, "A high-precision and high-robust LiDAR-inertial SLAM method suitable for robot operation scenarios." Jul. 23, 2025. doi: 10.21203/rs.3.rs-6565085/v1.
[23] X. Xu *et al.*, "A review of multi-sensor fusion SLAM systems based on 3D LiDAR," *Remote Sensing*, vol. 14, no. 12, p. 2835, Jun. 2022, doi: 10.3390/rs14122835.
[24] Z. Fan, L. Zhang, X. Wang, Y. Shen, and F. Deng, "Multi-sensor fusion simultaneous localization and mapping: a systematic review," 2024, [Online]. Available: https://www.researchsquare.com/article/rs-4922197/v1
[25] G. Qi, D. Ma, Y. Du, X. Cao, and H. Chen, "Research on SLAM of mobile robot based on fusion of laser and vision," in *Second International Conference on Electronic Information Engineering and Computer Communication (EIECC 2022)*, Mar. 2023, vol. 12594, p. 45. doi: 10.1117/12.2671329.
[26] S. Jin, Q. Meng, X. Dai, and H. Hou, "Safe-Nav: learning to prevent PointGoal navigation failure in unknown environments," *Complex & Intelligent Systems*, vol. 8, no. 3, pp. 2273–2290, Jun. 2022, doi: 10.1007/s40747-022-00648-2.
[27] C. Wang *et al.*, "Autonomous mobile robot navigation in uneven and unstructured indoor environments," in *2017 IEEE/RSJ International Conference on Intelligent Robots and Systems (IROS)*, Sep. 2017, vol. 2017-Septe, pp. 109–116. doi: 10.1109/IROS.2017.8202145.
[28] T. P. do Nascimento, P. Costa, P. G. Costa, A. P. Moreira, and A. G. S. Conceição, "A set of novel modifications to improve algorithms from the A* family applied in mobile robotics," *Journal of the Brazilian Computer Society*, vol. 19, no. 2, pp. 167–179, Jun. 2013, doi: 10.1007/s13173-012-0091-5.
[29] R. A. R. H. Kusuma *et al.*, "Collision avoidance for autonomous wheelchair using integrated SLAM and YOLO," in *2025 10th International Conference on Control and Robotics Engineering (ICCRE)*, May 2025, pp. 218–222. doi: 10.1109/ICCRE65455.2025.11093502.
[30] J. Cai, R. Yu, and L. Cheng, "Autonomous navigation research for mobile robot," in *Proceedings of the 10th World Congress on Intelligent Control and Automation*, Jul. 2012, vol. 29, pp. 331–335. doi: 10.1109/WCICA.2012.6357893.
[31] W. Sanboontho, A. Pichitkul, S. Tantrairatn, T. Phiboon, and A. Ariyarit, "Indoor localization and measurement object in field for TurtleBot using combined 2D-LiDAR and monocular camera," *Journal of Physics: Conference Series*, vol. 3022, no. 1, p. 012004, May 2025, doi: 10.1088/1742-6596/3022/1/012004.
[32] Z. Wei, S. Wang, K. Chen, and F. Wang, "ROS-based navigation and obstacle avoidance: a study of architectures, methods, and trends," *Sensors*, vol. 25, no. 14, p. 4306, Jul. 2025, doi: 10.3390/s25144306.

## BIOGRAPHIES OF AUTHORS

**Rifda Hakima Sari** is an Electronics and Instrumentation graduate (2022) and current master's student at Universitas Gadjah Mada, specializing in embedded systems, digital signal processing, and AI. Her background includes competing with UGM's Gamantaray autonomous ship team and contributing to major funded research projects, which have yielded numerous publications and intellectual property rights. She can be contacted at rifda.hakima.sari@mail.ugm.ac.id.

**Jazi Eko Istiyanto** is currently a full professor in Electronics and Instrumentation at Universitas Gadjah Mada, Faculty of Mathematics and Natural Sciences, a position he has held since 2010, before taking office at BAPETEN (Indonesia Nuclear Energy Regulatory Agency) as the Chairman from February 2014 until October 2021. Jazi Eko Istiyanto holds a Ph.D. (1995) in Electronic Systems Engineering, an M.Sc. (1988) in Computer Science, and a Postgraduate Diploma (1987) in Computer Programming and Microprocessors' Applications from the University of Essex, Colchester, United Kingdom, and a B.Sc. (1986) in Nuclear Physics from Universitas Gadjah Mada, Yogyakarta, Indonesia. His research interests cover embedded systems and cyber-physical systems security. He is also a registered engineer (electronic engineering) in Indonesia and the ASEAN countries. He can be contacted at jazi@ugm.ac.id.

**Oskar Natan** received the B.A.Sc. and M.Eng. degrees in Electronics and Electrical Engineering from Politeknik Elektronika Negeri Surabaya, Indonesia, in 2017 and 2019, and the Ph.D. degree in Computer Science and Engineering from Toyohashi University of Technology, Japan, in 2023. An Assistant Professor with the Department of Computer Science and Electronics at Universitas Gadjah Mada since 2020, his research focuses on sensor fusion, hardware acceleration, and end-to-end systems. He is a member of IEEE ITS, IEEE-RA, and IndoCEISS, and serves as a reviewer for high-impact venues including IEEE Transactions on Intelligent Vehicles, IEEE T-ITS, ICRA, and IROS. He can be contacted at oskarnatan@ugm.ac.id.

**Zaidan Hakim** is a graduate and current master's student in Electronics and Instrumentation at UGM, possessing deep expertise in embedded systems, robotics, and AI. His background in control systems was solidified as Captain of the GMRT Humanoid Robot Division, where he implemented complex motion algorithms like Inverse Kinematics and LQR. Currently, he researches cutting-edge technologies including AI-based UAV flight controllers, AMR navigation, and medical device cybersecurity, with scientific works published internationally. He can be contacted at zaidan.hakim24@mail.ugm.ac.id.

**Danang Lelono** has been a lecturer at the Department of Computer Science and Electronics, Universitas Gadjah Mada (UGM), since 1998. He earned his Undergraduate (1994), Master's (2000), and Ph.D. in Physics (2017) degrees entirely from UGM. His primary research interests span Instrumentation & Control, Smart Sensors, Intelligent Systems, and Embedded Systems. He remains actively engaged in teaching and contributing to scientific advancements in electronics and computer science. He can be contacted at danang@ugm.ac.id.

**Andi Dharmawan** was born in Surakarta, Indonesia, in 1984. He received his B.Sc. in Electronics and Instrumentation in 2006, M.Sc. in Computer Science in 2009, and Ph.D. in Computer Science in 2017, all from Universitas Gadjah Mada, Indonesia. From 2007 to 2009, he worked as a Research Assistant at the Department of Computer Science and Electronics, Universitas Gadjah Mada. Since 2009, he has been a faculty member at the same department, where he is also a part of the Embedded Systems and Robotics Laboratory. His research interests include control systems for robotics, autonomous unmanned systems, and advanced control system development. He can be contacted at andi_dharmawan@ugm.ac.id.